

Architecture and Performance Testing of a Software GPS Receiver for Space-based Applications^{1,2}

Kenn Gold and Alison Brown
NAVSYS Corporation
14960 Woodcarver Road
Colorado Springs, CO 80921
719-481-4877
kgold@navsys.com and abrown@navsys.com

Abstract—Space-based GPS technology presents significant challenges over Earth-based systems. These include visibility issues for rotating platforms and tracking of GPS satellites from spacecraft that are in higher orbits than the GPS, realtime resolution of carrier phase ambiguities, and different dynamics during various mission phases. NAVSYS has developed a software GPS receiver that makes use of 3-dimensional Digital Beam Steering technology and inertial aiding to address these issues. This approach offers several advantages including all around visibility for spinning satellites, tracking of weak GPS signals, reduction of multipath, and reprogrammability to accommodate different mission phases. Additionally, a suite of simulation tools based around the NAVSYS Matlab Toolbox and Advanced GPS Hybrid Simulation products have been built to allow testing for simulated space environments. The receiver architecture and test tools are described in this paper.

TABLE OF CONTENTS

1. INTRODUCTION	1
2. MISSION PHASES OF INTEREST.....	1
3. HIGH-GAIN ADVANCED GPS RECEIVER.....	2
4. SOFTWARE REPROGRAMMABLE GPS RECEIVER...	3
5. SIMULATION FOR THE SPACE ENVIRONMENT	4
6. MATLAB GPS TOOLBOX	5
7. ADVANCED GPS HYBRID SIMULATOR.....	5
8. INTERNAV SOFTWARE	7
9. IMU SIMULATION.....	7
10. ALL-AROUND SATELLITE VISIBILITY	8
11. HIGH GAIN SATELLITE TRACKING.....	10
12. CONCLUSION	12
REFERENCES	12

1. INTRODUCTION

NAVSYS Corporation has developed the design for a flexible, high performance Space-based Software GPS Receiver (SSGR), and is currently building an Engineering Development Unit to demonstrate its next generation capabilities for space applications. The SSGR will provide

a flexible, integrated precision navigation and attitude determination solution for space applications including Low Earth Orbit (LEO), highly eccentric orbit (HEO) and Geostationary Earth Orbit (GEO) missions. The ability to track low power GPS satellites will extend the use of GPS for precision navigation and timing, particularly for high altitude space missions (above the GPS satellite constellation). The SSGR will be suitable for supporting multiple space missions, including GPS metric tracking during launch, orbit determination during transfer to geostationary orbits, and high accuracy navigation, attitude control and timing. The flexibility of the SSGR design will allow it to be re-programmed for use in launch and orbit entry, station-keeping and autonomous orbit estimation applications.

In design of a space-based GPS receiver, the difficulty comes in testing, since the dynamics involved are radically different from anything achievable on the ground. The multi-element Advanced GPS Hybrid Simulation (AGHS) capability available at NAVSYS addresses many of these concerns. The AGHS generates simulated digital signal sets using profiles generated by NAVSYS' MATLAB® Signal Simulation capability, which is in turn driven by trajectory and attitude information generated with Satellite Tool Kit (STK). The AGHS can be used to generate digital representations for the GPS signals under the various scenarios for playback either into an RF Re-modulator or directly into the GPS receiver.

The NAVSYS MATLAB Toolbox has been augmented with various new tools to allow easy simulation of various space-based mission profiles. The new features include tools to determine the visibility and expected signal strength of GPS signals that will be received in each scenario and the ability to drive the AGHS under each of these scenarios. Orbit and attitude information is easily entered into the tool through a text-based file.

2. MISSION PHASES OF INTEREST

The SSGR is based on the NAVSYS High-gain Advanced GPS Receiver (HAGR) software reprogrammable receiver, and includes additional functionality to address various

¹ 0-7803-8155-6/04/\$17.00©2004 IEEE

² IEEEAC paper #1387, Version 4 Updated December 17, 2003

complications of space-based GPS usage. The receiver must have a capability to maintain lock through dynamic maneuvers both during launch and through orbit transitions. GPS visibility must be maintained even for spinning satellites and when the satellite is in higher than GPS orbit. These issues are addressed by adding inertial data to aid the GPS tracking and recovery during outages due to dynamics and with the use of beam steering capability. The Digital Beam Steering capability utilized in the SSGR allows for

the construction of a composite GPS signal from multiple non-coplanar antenna elements placed around the spacecraft. The beam steering/null forming functionality also allows for tracking of weak GPS signals (such as GPS sidelobes) from higher than GPS orbit.

Table 1 summarizes the enhancements that will be required for the SSGR and the testing that will be done for each mission phase.

Table 1 Testing for Various Mission Phases

Mission/ Capability	Launch & Orbit Entry	Station-keeping	Formation-Flying	Recovery & Landing
3-D Beam-steering	Maintains SV visibility at all attitudes	Provides gain towards GPS SVs	Provides gain towards GPS SVs	Maintains SV visibility at all attitudes
Inertial-aiding	High dynamic aided tracking for data continuity and navigation through SV outages	N/A	N/A	High dynamic aided tracking for data continuity and navigation through SV outages
Precision GPS Navigation	Provides high accuracy code/carrier observations for Wide Area Differential GPS (WADGPS) solution	Provides high accuracy code/carrier observations for WADGPS solution	Provides high accuracy code/carrier observations for Kinematic GPS (KGPS) solution	Provides high accuracy code/ carrier observations for WADGPS and KGPS solution
Attitude Determination	N/A	Provides interferometric attitude data from array	Provides interferometric attitude data from array	N/A

3. HIGH-GAIN ADVANCED GPS RECEIVER

NAVSYS' High-gain Advanced GPS Receiver (HAGR) [1] is a software reprogrammable, digital beam steering GPS receiver. The HAGR components are illustrated in Figure 1. With the HAGR digital beam steering implementation, each antenna RF input is converted to a digital signal using a Digital Front-End (DFE). The HAGR can be configured to operate with up to 16 antenna elements (L1 and L2) with the

antenna elements installed in any user specified antenna array pattern.

Each DFE board in the HAGR can convert signals from 8 antenna elements. The digital signals from the set of the antenna inputs are then provided to the HAGR digital signal processing cards. The HAGR can be configured to track up to 12 satellites providing L1 C/A and L1 and L2 P(Y) observations when operating in the keyed mode. The digital signal processing is performed in firmware, downloaded

from the host computer. Since the digital spatial processing is unique for each satellite channel, the weights can be optimized for the particular satellites being tracked. The digital architecture allows the weights to be computed in the HAGR software, then downloaded to be applied pre-correlation to create a digital adaptive antenna pattern to optimize the signal tracking performance.

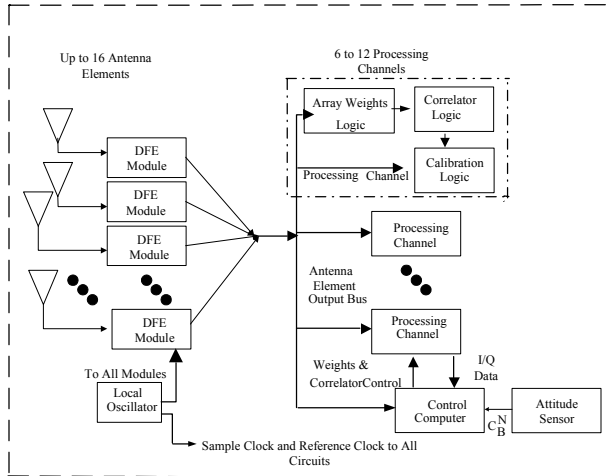


Figure 1 P(Y) HAGR System Block Diagram

4. SOFTWARE REPROGRAMMABLE GPS RECEIVER

The flexible Software GPS Receiver (SGR) architecture leveraged by the HAGR allows the GPS signal processing software and firmware to be easily ported to run on space qualified signal processing and host computer cards [2]. The GPS software radio architecture adopted by the HAGR shown in Figure 2 allows the receiver configuration to be optimized depending on the phase of flight [2]. For example, different antenna inputs and navigation modes could be used during launch and orbit entry than during the remaining mission life where the receiver could be optimized for autonomous orbit estimation and station keeping.

The SSGR Architecture utilizes 4-pi steridian field of view using 3-D digital beam steering providing continuous tracking during maneuvers while simplifying antenna installation through the use of a digital interface. Digital beam steering provides additive gain in the direction of the GPS satellite tracked improving signal reception at high altitude orbits (e.g. transfer orbits or GEO). Digital beam steering can provide antenna directivity towards both the GPS satellite main-lobes and side-lobes increasing the numbers of satellites that can be tracked. Modular digital beam-steering architecture can be configured for cross-strapping to provide added redundancy. Software reprogrammable GPS approach can be implemented on radiation hardened signal processors and re-used during the mission life to support multiple mission requirements.

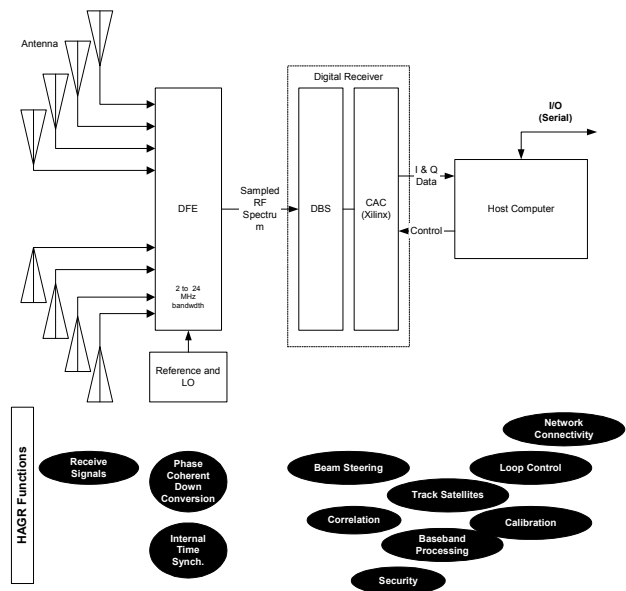


Figure 2 NAVSYS Software GPS Receiver Architecture

Digital Beam Steering

The digital signal from each of the HAGR antenna elements can be described by the following equation.

$$y_k(t) = \sum_{i=1}^{N_s} s_i(\underline{x}_k, t) + n_k(t) + \sum_{j=1}^{N_j} j_j(\underline{x}_k, t)$$

where $s_i(\underline{x}_k, t)$ is the i th GPS satellite signal received at the k th antenna element

$n_k(t)$ is the noise introduced by the k th DFE

$j_j(\underline{x}_k, t)$ is the filtered j th jammer signal received at the k th antenna element

The GPS satellite signal at each antenna element (\underline{x}_k) can be calculated from the following equation.

$$s_i(\underline{x}_k, t) = s_i(0, t) \exp\left\{-i \frac{2\pi}{\lambda} \underline{1}_i^T \underline{x}_k\right\} = s_i(0, t) e_{s_{ik}}$$

where $s_i(0, t)$ is the satellite signal at the array center and

$\underline{1}_i$ is the line-of-sight to that satellite

$e_{s_{ik}}$ are the elements of a vector of phase angle offsets for satellite i to each element k

The combined digital array signal, $z(t)$, is generated from summing the weighted individual filtered DFE signals. This can be expressed as the following equation.

$$z(t) = \underline{w}' \underline{y}(t) = \underline{w}' \left[\sum_{i=1}^{N_s} s_i(t) \underline{e}_{s_i} + \underline{n}(t) + \sum_{j=1}^{N_j} j_j(t) \underline{e}_{j_l} \right]$$

With beam steering, the optimal weights are selected to maximize the signal/noise ratio to the particular satellite being tracked. These are computed from the satellite phase angle offsets as shown in the following equation.

$$\underline{w}_{BS} = \begin{bmatrix} \exp\{-i\frac{2\pi}{\lambda} \underline{1}_i^T \underline{x}_1\} \\ \exp\{-i\frac{2\pi}{\lambda} \underline{1}_i^T \underline{x}_M\} \end{bmatrix} = \underline{e}_s$$

In Figure 3 and Figure 4 the antenna patterns created by the digital antenna array are shown for four of the satellites tracked. The HAGR can track up to 12 satellites simultaneously. The antenna pattern provides the peak in the direction of the satellite tracked (marked 'x' in each figure). The beams follow the satellites as they move across the sky. Since the L2 wavelength is larger than the L1 wavelength, the antenna beam width is wider for the L2 antenna pattern than for the L1.

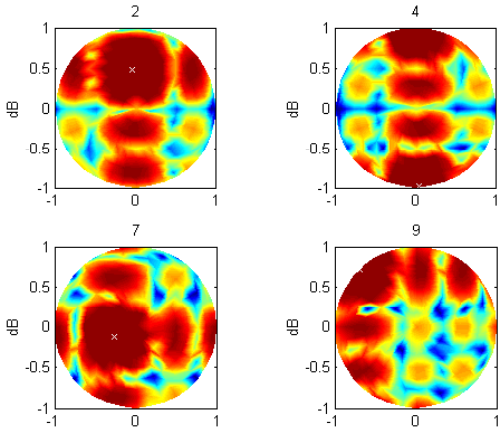


Figure 3 L1 Antenna Pattern

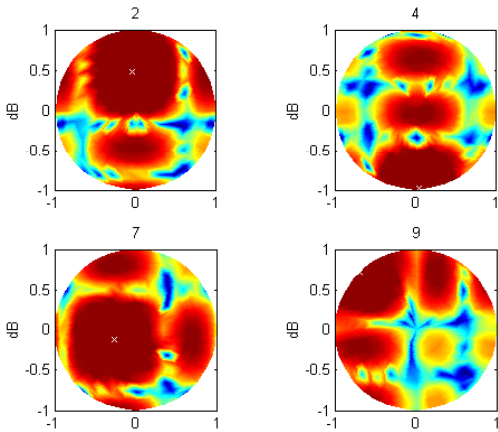


Figure 4 L2 Antenna Pattern

5. SIMULATION FOR THE SPACE ENVIRONMENT

The complex simulation environment that must be modeled for higher than GPS tracking is shown in Figure 5. The received signal power from the GPS satellites is a function of the GPS angle of directivity α . This must be computed based on the signal available from both the main lobes of the GPS satellite antenna pattern and the sidelobes, as shown in Figure 6. The model must also take into account earth blockage as well.

As an example, a plot of the user (Geostationary Operational Environment Satellite (GOES) and line-of-sight vectors to every available GPS satellite at the beginning of the simulation is shown in Figure 7 (Earth not to scale). Based on a minimum received C/No of 20 dB-Hz, seven GPS satellites were visible, which are shown in red (PRN 7, 8, 11, 13, 20, 22, and 27).

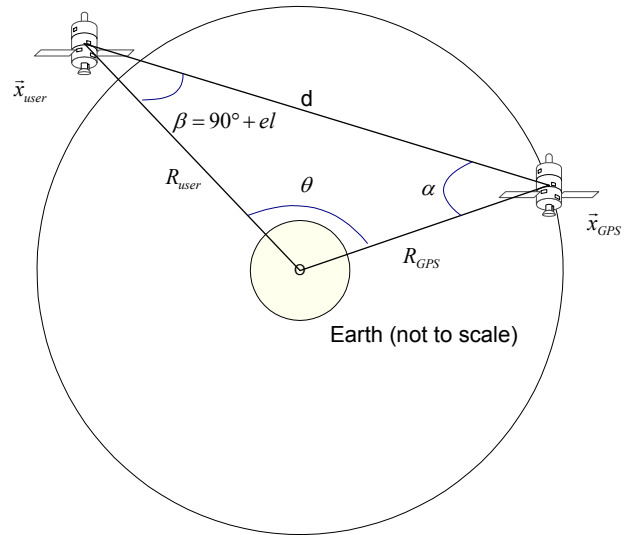


Figure 5 HEO orbit scenario

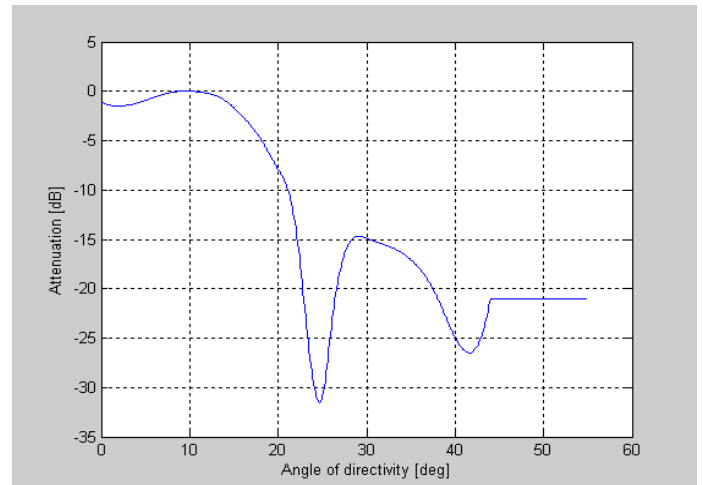


Figure 6 Modeled relative antenna attenuation of the GPS transmitting antennas

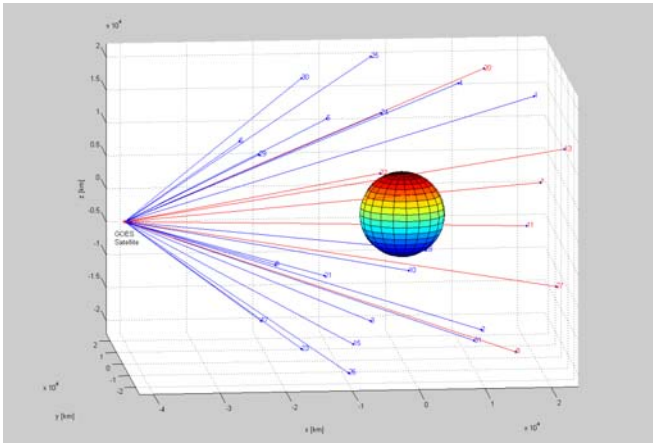


Figure 7 Line-of-sight vectors from GOES satellite to each available GPS satellite. Visible GPS satellites based on a C/No threshold of 20 dB-Hz are shown in red

6. MATLAB GPS TOOLBOX

The AGHS GPS signals are generated with inputs from the NAVSYS' Matlab GPS Tools. The signal flow employed in this generation process is shown in Figure 8. As the figure illustrates, the Matlab tools allow the user to have total control over the GPS signals that are simulated. The initial simulated trajectory is input as a user defined solution/trajectory profile.

The Matlab tools then convert this trajectory into an RNG format using the `sol2rng` function, which includes the pseudo-range, signal power, Doppler frequency shift and carrier phase of the simulated signals. The GPS navigation message data to be modulated on each simulated signal is also generated. The `aghssim` functions provide the low level control of the signal generation. This provides the raw signal amplitude and code phase and carrier phase information needed to generate the C/A and P(Y) code signals. There are two modes of operation for the `aghssim` functionality. The first is the software signal generation mode where the Matlab functions are used to directly generate a simulated Digital Signal File (DSF), which is a digital representation of the GPS simulated signals. The second mode is where the Correlator Accelerator Card (CAC) is controlled through the Matlab drivers to generate the digital simulated signal in real-time. In either of these modes, the AGHS generated signals can be recorded in the DSR and/or remodulated onto an RF carrier for output to a GPS receiver under test.

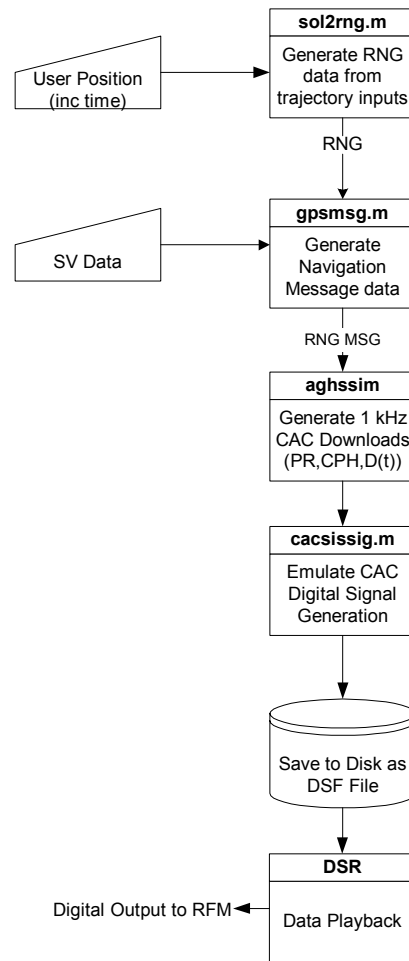


Figure 8 Signal Simulation Flowchart

7. ADVANCED GPS HYBRID SIMULATOR

The AGHS architecture is illustrated in Figure 9. This includes the following advantages over previous analog simulators that will be leveraged in the SSGR test activities.

- Access to all levels of satellite signal generator control through NAVSYS' Matlab satellite and signal generation scripts
- Software interface for insertion of future GPS signals or simulated jammer waveforms onto composite digital satellite signal profile.
- Digital data storage for exact reconstruction and playback of signal simulation profiles
- Digital output from the simulator of pre-recorded or real-time simulated signals
- Digital tracking of the recorded signals for high fidelity signal reconstruction and analysis
- High fidelity, phase coherent RF remodulation of digital signals for output to a GPS receiver or multi-element Controlled Reception Pattern Antenna (CRPA).

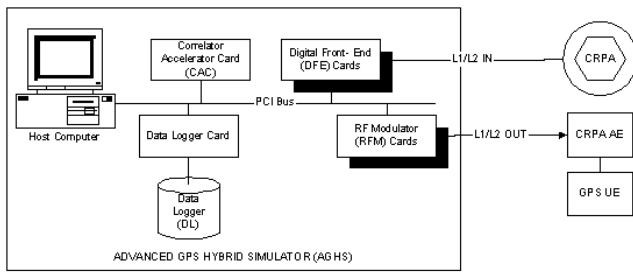


Figure 9 AGHS System Architecture

In the profile generation mode, the AGHS system generates the satellite signal profile to be simulated. The user trajectory is input either from a pre-defined solution file (SOL) or in real-time through the web interface.

Once the profile is defined, the AGHS system generates the digital simulated signals that emulate the digital outputs from each of the SSGR Digital Antenna Elements (DAEs) that would be applied to the SSGR signal processor. This mode will run in real-time and can also be used to generate recorded data files in the Data Logger (DL) subsystem for playback in the SSGR. We will record data libraries for each of the mission profiles generated to allow this testing to be repeated with different software configurations of the SSGR.

In the digital signal playback mode, the data recorded in the DSF is regenerated digitally for playback into the SSGR signal processor. As an option, it can also be modulated onto an RF signal by the RF Modulator (RFM) subsystem for playback into the individual antenna elements.

An Inertial Navigation System (INS) model component has also been added to the AGHS so we can generate simulated inertial-measurement unit (IMU) delta-theta and delta-V inputs into the SSGR during testing.

Satellite Tool Kit Interface

Satellite Tool Kit (STK) standard is the core of the STK software suite and it is free to all government, aerospace, and defense professionals. STK provides the analytical engine to calculate data and display multiple 2-D maps to visualize various time-dependent information for satellites and other space-related objects, such as launch vehicles, missiles, and aircraft. STK's core capabilities include orbit/trajectory ephemeris generation, acquisition times, and sensor coverage analysis for any of the objects modeled in the STK environment. To extend the analytical capabilities of STK, Analytical Graphics Inc. (AGI) also offers STK Professional (STK/PRO), a collection of additional orbit propagators, attitude profiles, coordinate types and systems, sensor types, inview constraints, and city, facility, and star databases.

Orbit trajectory generation is a feature included in the core STK program. Initial orbit state can be entered in Cartesian (Earth Fixed or Inertial) coordinates or with orbit Keplerian

elements. Many satellites are available in a database included with the program and others can be downloaded from the Analytical Graphics website. Several orbit integrators are available to generate the orbit trajectory from the initial state.

STK provides many visualization tools which are useful in determining that an orbit has been properly generated. Figure 10 shows a ground track for the MMS satellite, which is in a highly elliptic orbit. The apogee of this orbit is higher than the orbits of the GPS satellites.

Parameters for Highly-Eccentric-Orbit Satellite

Propagator:	TwoBody
Start Time:	24 Oct 2003 11:00:00.00 UTC
Stop Time:	25 Oct 2003 11:00:00.00 UTC
Step size:	60 sec
Orbit Epoch:	21 June 2003 00:00:00.00 UTC
Semimajor Axis:	41457.00 km
Eccentricity:	0.53846
Coord. Type:	Classical
Coord. System:	J2000
Inclination:	28.5 deg
Argument of Perigee:	0.0 deg
RANN:	90.0 deg
MEAN ANOMALY:	0.0 DEG

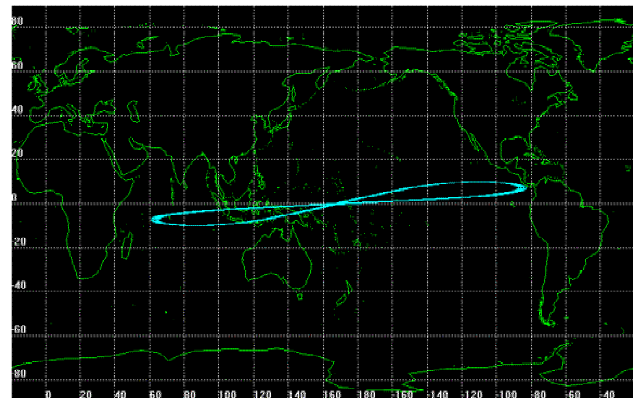


Figure 10 Groundtrack of HEO orbit

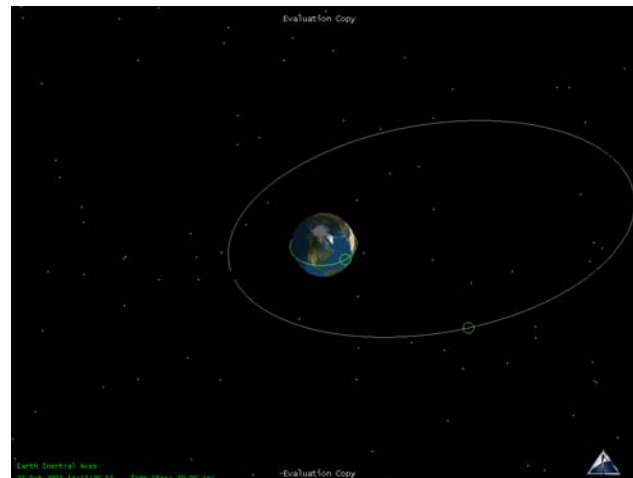


Figure 11 Highly Eccentric Orbit generated with STK

STK is capable of generating a report which contains the position and velocity of a satellite at user defined time steps. Figure 11 shows a portion of the trajectory generated in the Earth Centered Fixed coordinate frame at 10 sec intervals. This trajectory is used with a modified version of the sol2rng.m Matlab function to generate the range vectors and to drive the simulation for GPS data in orbital scenarios. Various attitude profiles are also available in the STK trajectory simulations, and attitude reports can be generated using Euler angles or quaternions. The modified AGHS simulation profiles make use of quaternions to describe the rotation of a satellite. The quaternions define the orientation of a vector in the spacecraft body-fixed frame with respect to the Earth Centered Inertial frame. Thus, a normal vector and in plane vector for a GPS antenna, defined in the Body fixed frame, relative to the spacecraft center of mass can be rotated to inertial coordinates. The GPS ToolBox contains functions to create a direction cosine matrix for this rotation from the quaternion set. The resulting vector can then be rotated to the ECF frame that describes the GPS orbits, allowing visibility and line of site calculations to be performed.

8. INTERNAV SOFTWARE

The NAVSYS InterNav software will be used to calculate combined GPS/Inertial navigation solutions. This includes the software functions illustrated in Figure 12. The receiver interface module handles the interface to the SSGR tracking software, which provides the GPS pseudo-range and carrier observations for processing in the Kalman Filter. The IMU interface module formats the IMU delta-theta and delta-V observation for the inertial navigation solution. The inertial navigation solution is based on a quaternion integration algorithm to compute the body-to-navigation transformation direction cosine matrix and integrate the acceleration to propagate position and velocity in a wander-azimuth navigation frame. The initialization and alignment procedure followed at start up is illustrated in Figure 13.

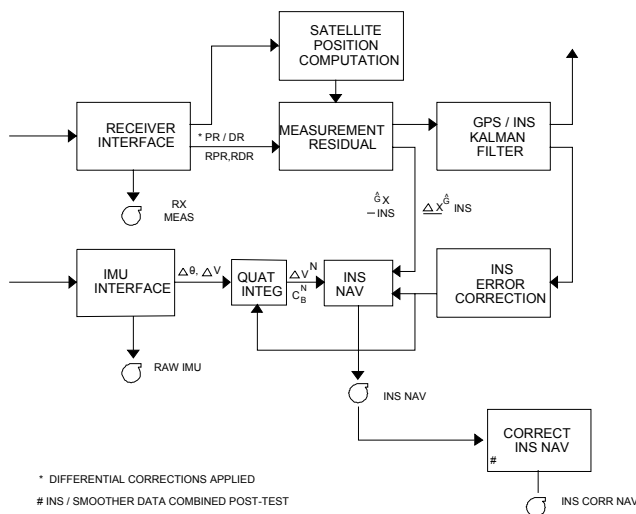


Figure 12 InterNav Software Architecture

In the rough leveling mode (system state=1), the GPS updates are used to estimate where the local level frame is. Once local level has been determined, the system transitions to the rough alignment mode (system state=2) to generate an initial estimate of the wander azimuth angle (and heading). Once the heading of the INS has been observed, the system transitions to the navigation mode (system state=3) where the accelerometer and gyroscope errors are further refined using a small-angle model for the Kalman Filter.

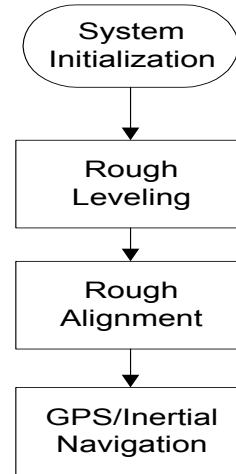


Figure 13 InterNav System Modes

The InterNav software will be integrated with the SSGR navigation software generating a tightly integrated GPS/inertial navigation solution and attitude data, which is used by the digital beam-steering software module. The inertial position, velocity, acceleration and attitude data will also be provided to the GPS tracking loops to be used for optimizing satellite selection and also aiding the tracking loops during high dynamics to minimize signal drop-out times.

9. IMU SIMULATION

To support future applications involving tightly integrated GPS and inertial systems and ultra-tightly-coupled GPS/inertial receivers, the AGHS has been upgraded to add inertial simulator capability. This will operate in conjunction with the AGHS satellite signal simulation capability as shown in Figure 14.

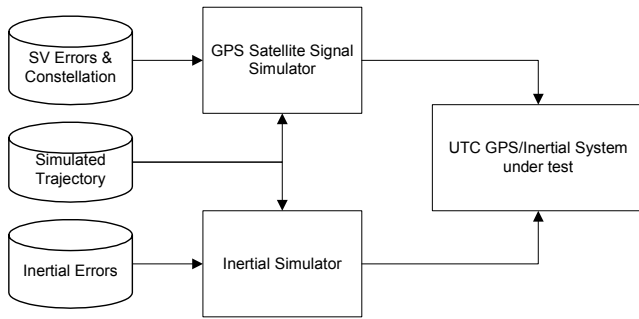


Figure 14 IMU Simulation Architecture

For this launch, the trajectory duration is approximately 10.2 minutes. In order to make the launch more applicable and realistic, a 20-second stationary data is added to the beginning of trajectory to simulate the initial position of the launch. This is necessary for two reasons: (1) making sure that IMU is in final alignment before initiating the launch and (2) verifying singularity does not occurred in IMU simulation by inspecting the final results. By the end of the launch window, the final altitude of the orbiter is 1,500 km, which places the vehicle in Low-Earth-Orbit. Figure 15 shows the flight path.



Figure 15 Vehicle Launch Path

Note in Figure 16 the sharp drop-off in roll is due to realignment of the space vehicle and not obvious. Figure 17 shows the difference between the input attitude and the corrected navigation attitude.

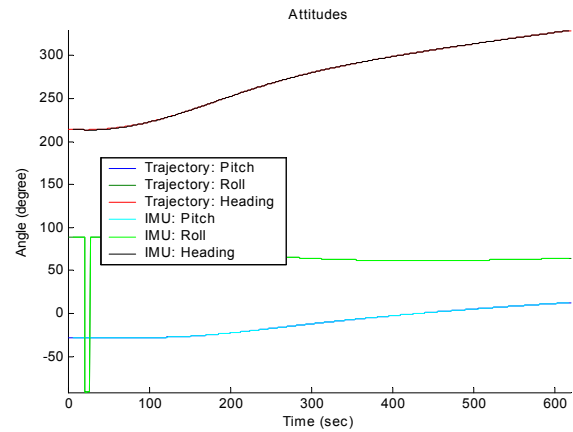


Figure 16 Attitude Plot of Trajectory and Corrected Navigation Data

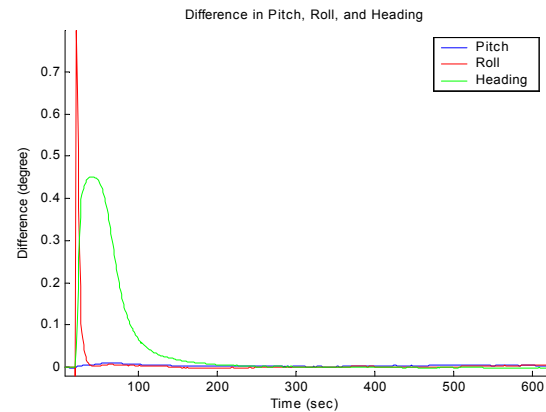


Figure 17 Difference in Trajectory and Corrected Navigation Data

In transient state, the attitude difference is in the order of tenths of a degree. The attitude error shows a convergence toward zero as the solution difference approaches steady-state response. With 20-second initial stationary trajectory, no singularity is observed and, in addition, the output shows an improvement over results without stationary initial position (not plotted here). With perfect initialization, the simulation provides expected results for corrected navigation position, altitude, and attitude.

10. ALL-AROUND SATELLITE VISIBILITY

Testing was completed to demonstrate the capability of the HAGR to provide all-around satellite visibility using multiple antenna elements. This testing was performed to show that a composite signal could be formed from the multiple elements. The test configuration is shown in Figure 18 and a picture of the test fixture is shown in Figure 19.

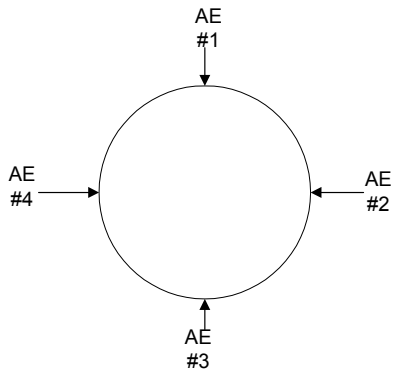


Figure 18 Four-Element All-around Visibility Antenna Testing



Figure 19 Satellite Test Fixture

Table 2 All-around Satellite Visibility Test Data Summary

PRN	AZ	EL	C/N0
1	155	23	42
2	245	19	44
3	55	31	48
7	205	13	39
8	305	13	-
10	311	10	-
11	125	10	37
13	294	51	45
15	98	12	43
18	189	60	47
19	341	72	44
27	305	45	46
31	100	53	47

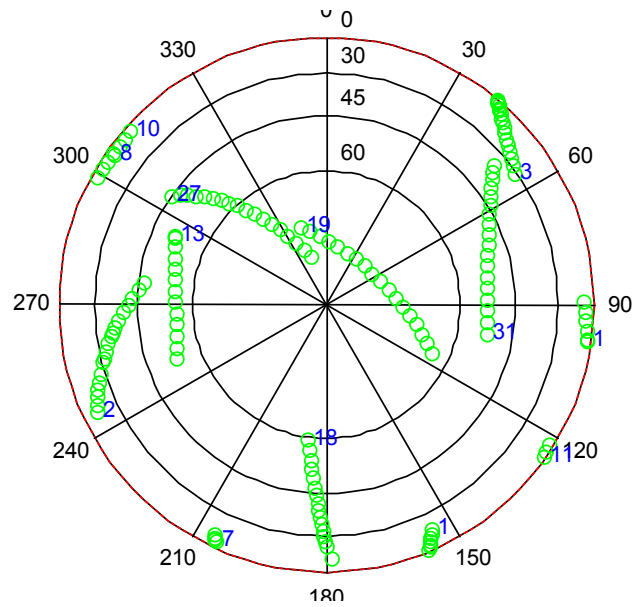


Figure 20 Skyplot of 3-D Beam steering Satellite Visibility

In Figure 20, a sky plot is shown with the locations of the GPS satellites tracked during the test. In Figure 21, the satellites (identified by PRN number) that were tracked during the test are plotted against time, and in Table 2, the signal-to-noise ratios of the satellites tracked during the test are listed. From this test data, it is evident that the 3-D beam forming is functioning correctly. All of the satellites above the horizon were tracked with the exception of satellites 8 and 10, which were not selected by the 8-channel GPS receiver. The signal-to-noise ratio is also comparable with normal GPS operation indicating no noticeable degradation from the 4π steridian signal combining.

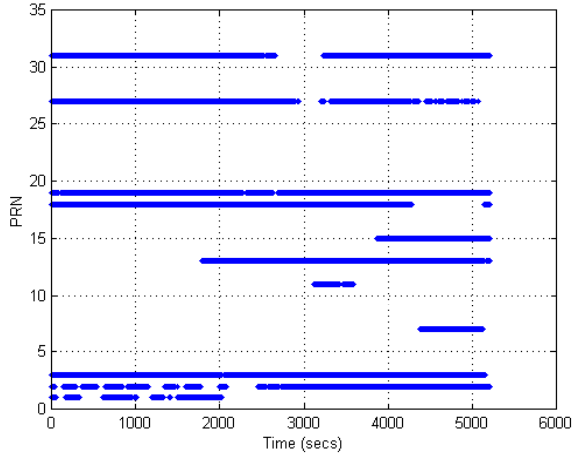


Figure 21 All-around Visibility Tests - SVs tracked

11. HIGH GAIN SATELLITE TRACKING

The directivity of the digital beam forming provides gain in the direction of the GPS satellites. This improves the ability of the digital beam steering receiver to be able to track GPS satellites with low signal power, for example, from a space platform located above the GPS satellite constellation. With a 16-element array, the beam steering provides up to 12 dB of additional gain. With a 7-element array, up to 8.45 dB of additional gain is provided. A data set was collected to observe the signal-to-noise ratio on the C/A and P(Y) code HAGR data over a period of 12 hours. From this data (Figure 22 and Figure 23), it can be seen that the beam steering increases the GPS signal strength to a value of 56 dB-Hz on the C/A code. As expected the P(Y) code observed signal strength is 3 dB lower.

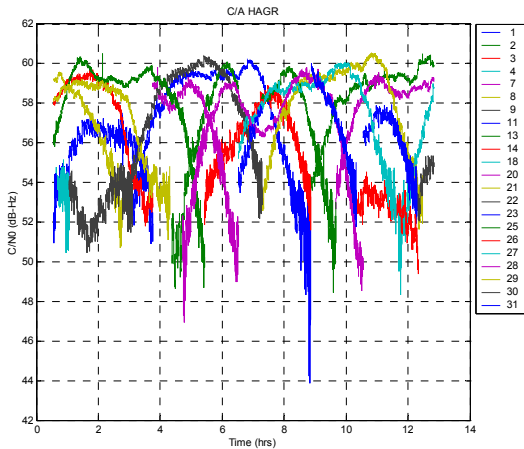


Figure 22 C/A HAGR Signal-to-Noise (dB-Hz)

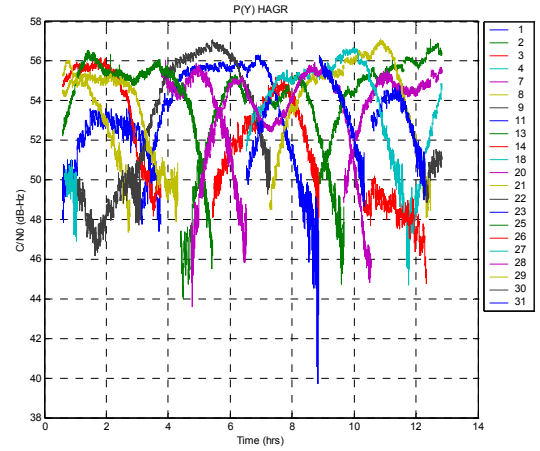


Figure 23 P(Y) HAGR Signal-to-Noise (dB-Hz)

Measurement Noise And Multipath Error Reduction

The digital beam steering also improves the measurement accuracy and decreases the effect of multipath errors from signal reflections received from the spacecraft structure (e.g. solar panels or antenna arrays).

The GPS L1 pseudo-range and carrier-phase observations are described by the following equations.

$$PR_{i1}(m) = R_i + b_u + I_i + \Delta_{Ti} + \tau_{M1i} + n_{PR1}$$

$$CPH_{i1}(m) = N_1 \lambda_1 + n_{CPH1} - (R_i + b_u - I_i + \Delta_{Ti} + \lambda_1 \theta_{M1i})$$

The following errors affect the pseudo-range and carrier phase observations.

- Ionosphere errors– (I)
- Troposphere errors – these are the same on all of the observations (Δ_{Ti})
- Receiver Measurement Noise – these are different on each of the observations (n_{PR1}, n_{CPH1})
- Multipath Noise – these are different on each of the observations ($\tau_{M1i}, \lambda_1 \theta_{M1i}$)
- Satellite and Station Position error - these affect the ability to correct for the Range to the satellite (R_i)
- Receiver clock offset (b_u)

From this equation, the L1 pseudo-range + carrier phase sum cancels out the common errors and the range to the satellite and observes the pseudo-range and multipath errors as well as the change in the ionospheric offset.

$$PR_{i1} + CPH_{i1}(m) = 2I_i + \tau_{M1i} + n_{PR1} + N_1 \lambda_1 + n_{CPH1} - \lambda_1 \theta_{M1i}$$

$$= C + 2I_i + \tau_{M1i} + n_{PR1} + (n_{CPH1} - \lambda_1 \theta_{M1i})$$

$$\approx C + 2I_i + \tau_{M1i} + n_{PR1}$$

The PR+CPH is plotted in Figure 25 for SV 25 and each of the receiver data sets. The short term (<100 sec) white receiver noise was removed by passing the PR+CPH

observation through a linear filter. The drift caused by the ionosphere on each observation was removed using a polynomial estimator. The remaining cyclic error is an estimate of the multipath pseudo-range errors. The RMS white noise on the pseudo-range observations was computed by differencing the PR+CPH measurement. This is shown in Figure 26 and Figure 27 for all of the satellites tracked for the C/A and P(Y) code observations. The observed PR noise shows good correspondence with the predicted values, based on analysis of the tracking loops, shown in Figure 28. For C/N0 values above 52 dB-Hz, the P(Y) code HAGR provided pseudo-range accuracies of 5 cm (1-sigma) while for C/N0 values above 55 dB-Hz the C/A code observations were accurate to 15 cm. These values are for 1-Hz observations without any carrier smoothing applied. The mean observed RMS accuracies are summarized below in Table 3 with the average peak multipath PR errors observed.

The short term cyclic variations shown in Figure 25 are caused by multipath errors. The peak-to-peak cyclic PR variation for each of the receiver data sets was calculated to estimate the errors observed for each satellite from the pseudo-range multipath^[1]. These errors are listed in Table 3 for each of the satellites. The HAGR spatial signal processing can also be used to detect the presence of multipath and adapt the antenna pattern to further minimize these errors[3,4]. In Figure 24 spatial information from a 7-element phased array is shown that identifies the source of a strong multipath signal through direction of arrival (DOA) estimation using the MUSIC algorithm[5]. Testing has shown that the digital beam steering and spatial processing significantly reduces the multipath errors on the carrier phase observations. This is important for space applications which rely on the GPS carrier phase information, such as interferometric attitude determination.

Table 3 Mean PR Noise and M-path Peak Errors (m) (16-element array)

SVID	C/A HAGR RMS PR	C/A Mean Mpath PR	P(Y) HAGR RMS PR	P(Y) Mean Mpath PR
1	0.239	0.259	0.054	0.202
3	0.284	0.494	0.056	0.337
8	0.200	0.278	0.045	0.202
11	0.278	0.535	0.059	0.287
13	0.252	0.321	0.059	0.260
14	0.214	0.359	0.049	0.350
20	0.222	0.267	0.050	0.164
21	0.252	0.261	0.058	0.133
22	0.248	0.318	0.047	0.217
25	0.202	0.362	0.044	0.265
27	0.183	0.270	0.044	0.178
28	0.236	0.366	0.055	0.272
29	0.225	0.312	0.050	0.217
30	0.477	0.791	0.089	0.624
31	0.325	0.266	0.055	0.135

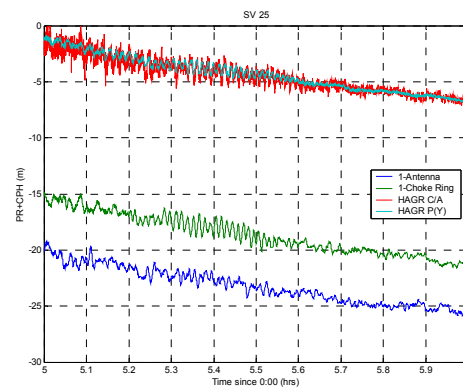


Figure 25 PR+CPH (m) - SV 25

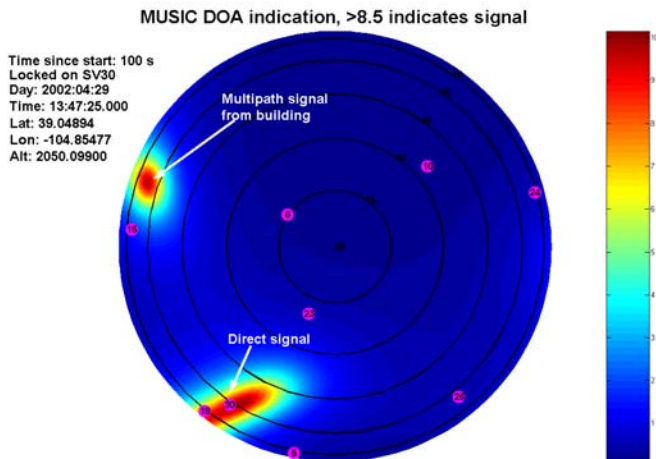


Figure 24 MUSIC direction of arrival estimation

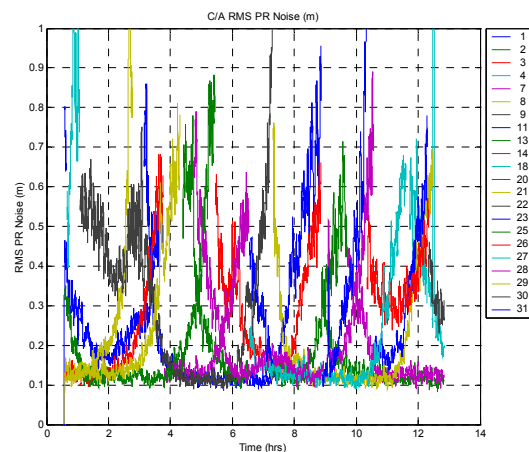


Figure 26 HAGR C/A Code Pseudo-Range Noise (m) (16-element array- no carrier smoothing)

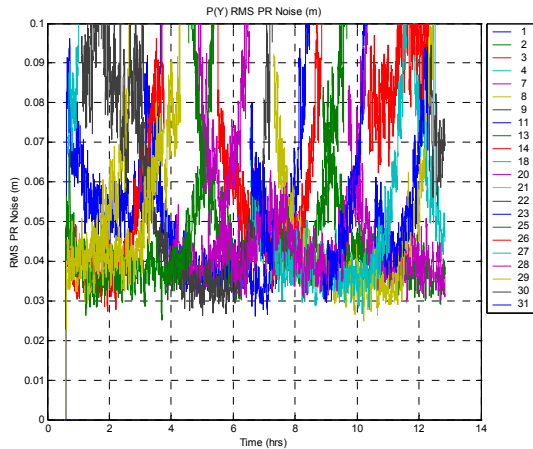


Figure 27 HAGR P(Y) Code Pseudo-Range Noise (m) (16-element array– no carrier smoothing)

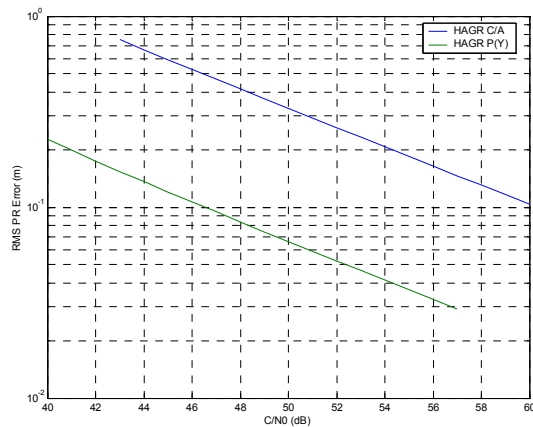


Figure 28 C/A and P(Y) HAGR RMS PR error versus C/N0

12. CONCLUSION

The test data presented in this paper has shown that the digital beam steering architecture has advantages in: increasing the received GPS signal/noise ratio, which improves the tracking performance for low power satellite signals; improving the measurement accuracy for precision applications such as rendezvous, docking or formation flying; minimizing carrier phase multipath errors which can result in improved interferometric attitude determination.

NAVSYS is currently developing a design for a space-borne version of our reprogrammable, digital beam steering GPS receiver product under contract to AFRL/VS and NASA Goddard Space Flight Center (GSFC). This modular, flexible architecture is designed to be ported from our in-house test-bed to a variety of space-qualified signal processing boards and host computers to provide an embedded GPS capability. The design also allows the receiver to be reconfigured in-flight to optimize the GPS tracking performance depending on the needs of each phase of the mission.

To aid in testing of this space qualified receiver, the NAVSYS GPS Toolbox, and AGHS products have been augmented to include tools to allow simulation of GPS data in a space environment. In addition, the IMU simulation of the InterNav product has also been incorporated into the AGHS design.

REFERENCES

- [1] A. Brown, N. Gerein, "[Test Results from a Digital P\(Y\) Code Beamsteering Receiver for Multipath Minimization](#)," ION 57th Annual Meeting, Albuquerque, NM, June 2001.
- [2] N. Gerein, A. Brown, "[Modular GPS Software Radio Architecture](#)," Proceedings of ION GPS 2001, Salt Lake City, Utah, September 2001.
- [3] A. Brown, "[Performance and Jamming Test Results of a Digital Beamforming GPS Receiver](#)," Joint Navigation Conference, Orlando, FL, May, 2002.
- [4] D. Sullivan, R. Silva, and A. Brown, "[High Accuracy Differential and Kinematic GPS Positioning using a Digital Beam Steering Receiver](#)," Proceedings of 2002 Core Technologies for Space Systems Conference, Colorado Springs, CO, November 2002.
- [5] A. Brown and K. Stolk; "[Rapid Ambiguity Resolution using Multipath Spatial Processing for High Accuracy Carrier Phase](#)," Proceedings of ION GPS 2002, Portland, OR, September 2002.

BIOGRAPHY

Kenn Gold is a Product Area Manager at NAVSYS Corporation for the Advanced Systems and Simulation Tools group. His work includes development of spaceborne GPS receivers, integrity monitoring algorithm development, and GPS simulator design. He holds a PhD from University of Colorado in Aerospace Engineering.



Alison Brown is the President and Chief Executive Officer of NAVSYS Corporation. She has a PhD in Mechanics, Aerospace, and Nuclear Engineering from UCLA, an MS in Aeronautics and Astronautics from MIT, and an MA in Engineering from Cambridge University. In 1986, she founded NAVSYS Corporation. Currently she is a member of the GPS-III Independent Review Team and Scientific Advisory Board for the USAF and serves on the GPS World editorial advisory board.



ACKNOWLEDGEMENTS

This work is being sponsored under an SBIR contract to AFRL/VS and to NASA GSFC. The authors would like to express their appreciation for the support of these organizations and the technical points of contact, Dr. Alan Lovel and Dr. Michael Moreau, in the development of this new technology.